$N_{4,5}OO$ resonance Auger spectra of Xe studied with selective excitation by synchrotron radiation

H. Aksela,* S. Aksela,* G. M. Bancroft, and K. H. Tan
Centre for Chemical Physics, University of Western Ontario, London, Ontario, Canada N6A 3K7 and Canadian Synchrotron Radiation Facility, Synchrotron Radiation Center, University of Wisconsin, Stoughton, Wisconsin 53589

H. Pulkkinen
Department of Physics, University of Oulu, SF-90570 Oulu 57, Finland
(Received 8 July 1985; revised manuscript received 21 January 1986)

The high-resolution $N_{4,5}OO$ normal Auger spectrum and resonantly excited Auger and autoionization spectra of Xe have been investigated using synchrotron radiation to ionize or excite the $4d$ levels. Excitation of the $4d$ electrons to the $4d^9 5s^2 5p^6 6p$ resonance states results in the decay processes with a $6p$ spectator or participator electron. Besides the previously reported strong resonance Auger peaks, the whole resonance Auger spectrum has been studied in detail. Energies and intensity distributions of different processes are calculated and compared with experiment.

INTRODUCTION

High-energy electron beam excitation has been used to create the high-resolution $N_{4,5}OO$ Auger spectrum of Xe reported by Werme *et al.*[1] and Aksela *et al.*[2] These spectra contain, besides the $N_{4,5}OO$ lines, many satellite lines originating from ionization of deeper core levels. These often decay via $XN_{4,5}Y$ Auger transitions, which as the next step give $N_{4,5}YOOY$ satellites which accompany the $N_{4,5}OO$ transitions on their low-kinetic-energy side. Therefore, for the investigation of weaker lines and correlation satellites in the $N_{4,5}O_1O_{2,3}$ group, monochromatic and tunable synchrotron radiation provides a unique excitation method. An $N_{4,5}OO$ Auger spectrum of Xe excited by photon energy $h\nu=94$ eV has already been reported by Yates *et al.*[3] in connection with their study of $4d$ photolines, but no detailed analysis for the $N_{4,5}OO$ spectrum was given. A part of the spectrum was also presented by Southworth *et al.*[4]

The resonance excitation of the $4d$ electrons to empty np ($n=6,7$) levels provides the second interesting field of study. The first such study for xenon was reported by Eberhardt *et al.*[5] and later by Schmidt *et al.*[6] Very recently Southworth *et al.*[4] have also published some resonance Auger spectra for Xe. These studies,[4-6] however, have been either limited only to the strongest part of the $N_{4,5}OO$ Auger spectrum,[5,6] or the resolution has not been high enough[4] to reveal detailed fine structure of the spectra. Also, these papers have not given any detailed analysis, like a comparison with calculations, for the spectra. For these reasons we have undertaken to investigate thoroughly the electron spectrum of Xe with high resolution using synchrotron radiation.

The postcollision interaction (PCI) studied in recent papers[4,6] is left outside the scope of this work. We thus focus on those transitions which occur after ionization reasonably far from threshold, or excitations to well-isolated resonance states.

EXPERIMENTAL

The experimental measurements were made by using the Canadian Synchrotron Radiation Facility designed for the Aladdin storage ring presently under construction and mounted now on the Tantalus storage ring in Stoughton, Wisconsin. The beam line and its Mark IV Grasshopper monochromator have been described elsewhere.[3,7] A monochromator resolution of 2 Å was used for the resonance Auger spectra, resulting in a photon linewidth of 0.6 eV at ~60-eV photon energies. The Leybold-Heraus LHS-11 system was used as the electron spectrometer. The analyzer was mounted at the magic angle (54.7°) so that electron intensities are dependent of β and the polarization of the incident radiation. The analyzer works in the constant-pass-energy mode with the result that the analyzer transmission function is independent of the initial kinetic energy.[3] This is an essential advantage when very-low-energy Auger lines are studied. All spectra were obtained by 50-eV pass energies resulting in total Auger linewidths of ≤ 0.4 eV.

Figure 1(a) shows the entire normal $N_{4,5}OO$ Auger electron spectrum of Xe measured using 114 eV photon energy to ionize the $4d$ levels. Figures 1(b) and 1(c) show the resonantly excited N_5OO and N_4OO Auger and autoionization spectra of Xe, created by 65.3- and 67.3-eV photons exciting the $4d_{5/2}$ and $4d_{3/2}$ electrons, respectively, to the $6p$ Rydberg states. Figure 2 shows the $5s$ photoelectron spectrum of Xe taken at 72.5 eV photon energy. This spectrum overlaps the resonance Auger spectra [Figs. 1(b) and 1(c)]. The high-kinetic-energy peak in both spectra is the most intense $5s$ peak. Energy calibration was carried out with the aid of the $N_4O_{2,3}O_{2,3}(^1D_2)$ and $N_4O_1O_{2,3}(^1P_1)$ Auger lines of Xe with energies of 34.31 and 21.67 eV, respectively.[2] The experimental $N_{4,5}O_{2,3}O_{2,3}$ spectrum [Fig. 3(a)] was fit with the use of the computer code CRUNCH.[8] The width and the shape of the Voigt function from the experimental fit of a peak

known from theory to be a single line was used to form the theoretical profiles.

DISCUSSION

Normal $N_{4,5}OO$ Auger spectra

High-energy electron-beam-excited $N_{4,5}OO$ Auger spectra of Xe have recently been studied and compared with the relativistic multiconfiguration calculations for the transition energies.[2] The $N_{4,5}OO$ Auger spectrum taken with 114-eV photons [Fig. 1(a)] agrees well with the earlier measurements,[1,2] but shows the main line structures in more detail, because part of the complicated satellite structure present in the electron-beam-excited spectrum is now absent. In this work we also have carried out calculations for both energies and the transition probabilities, and thus a direct comparison between experimental and calculated profiles become possible.

Such a comparison for the $N_{4,5}O_{2,3}O_{2,3}$ transitions is given in Fig. 3. The energies for the theoretical profile are computed with the MCDF code of Grant *et al.*[9] and the intensities are obtained with the use of the radial integrals tabulated by McGuire.[10] The general agreement between experiment and theory is reasonably good. The calculated

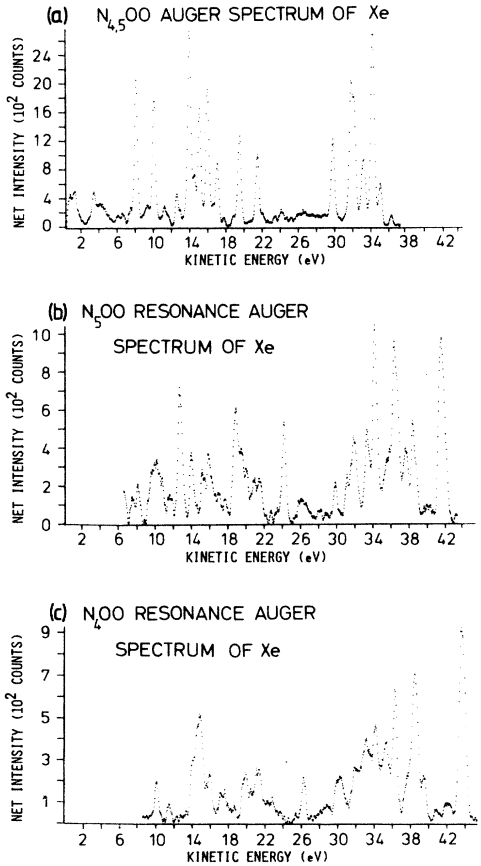

FIG. 1. Auger and resonance Auger electron spectra of Xe recorded using (a) 114-eV photons to ionize the $4d$ electrons, (b) 65.3-eV photons to excite the $4d_{5/2}$ electrons to the $6p$ Rydberg states, (c) 67.3-eV photons to excite the $4d_{3/2}$ electrons.

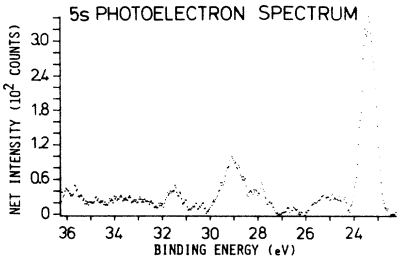

FIG. 2. $5s$ photoelectron spectrum of Xe taken at 72.5 eV photon energy. This spectrum has been subtracted from the $N_5O_{2,3}O_{2,3}$ and $N_4O_{2,3}O_{2,3}$ resonance Auger spectra [Figs. 5(b) and 6(b)].

energy splitting is, however, slightly overestimated, as pointed out already in Ref. 2. Due to this overestimation, calculated $N_5O_{2,3}O_{2,3}(^1D_2)$ and $N_4O_{2,3}O_{2,3}(^1S_0)$ lines are well separated, whereas the experimental ones overlap more strongly. For example, the strongest overlap occurs in the case of the $N_5O_{2,3}O_{2,3}(^3P_2)$ and $N_4O_{2,3}O_{2,3}(^1D_2)$ lines in the experimental spectrum. The determination of their individual line intensities is thus very difficult and the fit presented in Fig. 3(a) should not be taken too literally. Comparison between calculated and experimental intensities indicates that the intensities of the $^1S_0$ lines are underestimated and the intensities of the $^1D_2$ lines probably overestimated by theory. Only the single-configuration computations were performed in the present case. Correlation is neglected in these calculations, and it plays the strongest role in the case of the $^1S_0$ lines. Figure 3 thus displays the degree of the agreement with theory using the single-configuration description. Figure 3 serves

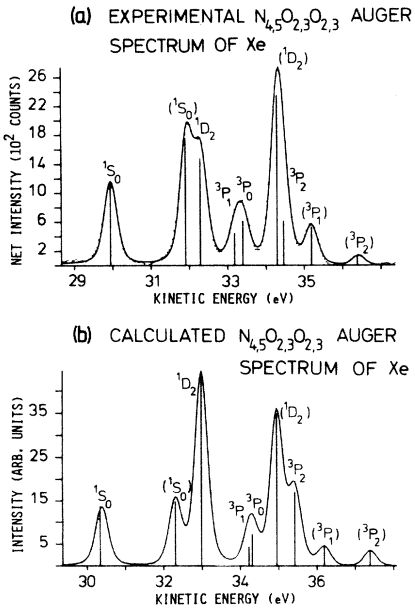

FIG. 3. Comparison between (a) experimental and (b) calculated $N_{4,5}O_{2,3}O_{2,3}$ Auger electron spectra. LS symbols in parentheses refer to the N_4 group and those without brackets to the N_5 group.

as a reference for the resonance Auger spectra presented in the next section. When forming the theoretical profile in Fig. 3, the statistical N_5:N_4 branching ratio was used. Assuming 1:1 decomposition between the overlapping $N_4O_{2,3}O_{2,3}(^1D_2)$ and $N_5O_{2,3}O_{2,3}(^3P_2)$ lines, we obtain the experimental value of 1.3 for the $I_{N_5O_{2,3}O_{2,3}}$:$I_{N_4O_{2,3}O_{2,3}}$ ratio. This is in agreement with Ref. 1, and shows that there is an additional disagreement between experimental and calculated profiles in Fig. 3. Outer-shell Auger spectra on Ne and Ar were also found[1] to deviate from the statistical branching ratio.

Before discussing the more complex Auger profiles in Fig. 4, it is important to introduce the different terminology used to discuss the satellites in Fig. 2. The strong satellite structure associated with ionization in the outer s shell of the heavier rare gases has been the subject of many photoelectron studies.[11–17] The satellites are caused by an Auger-like process in which the $5s$ hole state is filled by a $5p$ electron with simultaneous excitation of another $5p$ electron to a $5d$ or $6s$ state:

$$5s^15p^6 \leftrightarrows 5s^25p^4 \begin{cases} 5d^1 \\ 6s^1 \end{cases} . \quad (1)$$

The process is usually discussed in terms of configuration interaction (CI),[13,15–17] and rarely referred to as an Auger or Coster-Kronig transition.[11] This is because the CI approach, by diagonalizing the matrix coupling the $5s^15p^6$ and $5s^25p^45d^1,6s^1$ configurations, is well suited for describing energy shifts and transfer of intensity to satellite lines. These satellites are often called correlation satellites to distinguish them from the shake-up satellites, which originate when an outer electron is shaken up in the presence of an inner-shell ionization.

Next we compare the calculated and experimental $N_{4,5}O_1O_{2,3}$ profiles. For this group, the normal Auger lines [Fig. 4(a)] are shifted and accompanied on their low-energy side by satellite lines as can be seen by the experimental spectrum in Fig. 4(d). An analogous assignment to (1) for the satellites would be a double Auger process where the final state of the Auger transition further Auger decays, resulting in the excitation of the second Auger electron to a Rydberg state:

$$4d^95s^25p^6 \rightarrow 4d^{10}5s^15p^5 \leftrightarrows 4d^{10}5s^25p^3 \begin{cases} 5d^1 \\ 6s^1 \end{cases} . \quad (2)$$

In the language of CI we are considering a strong mixing of the $5s^15p^5$ configuration with the $5s^25p^35d^1$ and $5s^25p^36s^1$ configurations, so that the $5s^15p^5$ Auger strength is spread over the many states that result from these configurations. The calculated profiles corresponding to a single-configuration picture and a multiconfiguration picture, discussed in more detail below, are shown with the experimental $N_{4,5}O_1O_{2,3}$ spectrum in Fig. 4.

When the Ar, Kr, and Xe photoelectron spectra are compared with each other, the increase in the correlation satellite intensity proceeding from Ar to Kr and further to Xe is nicely demonstrated.[12,13] Furthermore, a strong increase in the intensity of these satellites is observed in going from a single-hole state $5s^15p^6$ to a double-hole state $5s^15p^5$ present in the final state of the $N_{4,5}O_1O_{2,3}$ Auger transitions. This can been seen from comparison of Fig. 2 (where the $5s^15p^6$ satellites can be seen in the high-binding-energy region) with Fig. 4(d) (where the very intense $5s^15p^5$ satellites can be seen in the low-kinetic-energy regions). This clearly indicates that the correlation effects are very sensitive to the degree of the ionization and the states of the other electrons in an atom. In order to obtain the redistribution of the intensity due to the interaction between the $5s^15p^5$ and $5s^25p^35d^1$ final states of the Auger transitions, we have carried out calculations of the transition probabilities by using as the final-state wave functions the linear combinations of the wave functions of the correlating $5s^15p^5$ and $5s^25p^35d^1$ states, as obtained from energy calculations carried out by the MCDF code of Grant.[9] Only the $5s^25p^35d^1$ states most strongly mixed with $5s^15p^5$ were taken into account in carrying out the

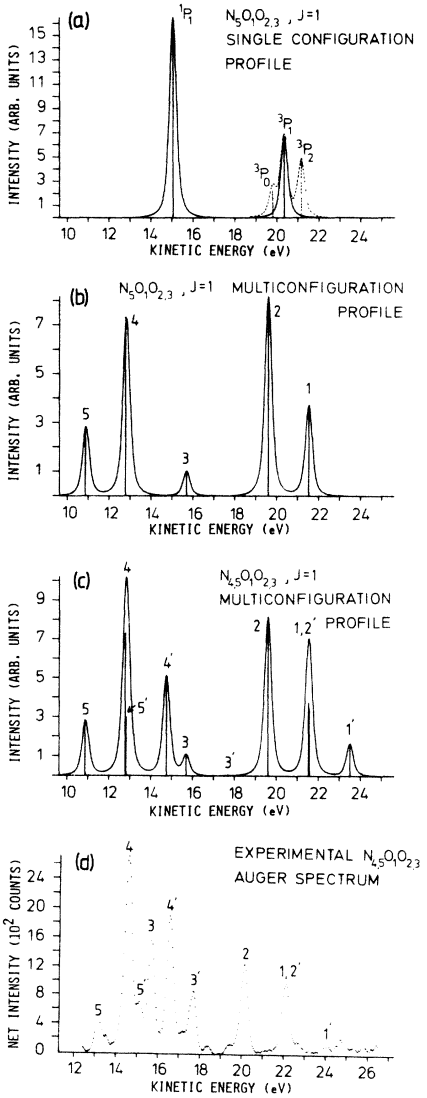

FIG. 4. Comparison between calculated (a) single-configuration, and (b) and (c), multiconfiguration profiles with the experimental $N_{4,5}O_1O_{2,3}$ Auger spectrum. (d) Numbered peaks are discussed in the text.

multiconfiguration computations. As pointed out by Smid and Hansen,[16] a good description in the case of the photoelectron spectrum was obtained with the use of a multiconfiguration computation where higher Rydberg states as well as the continuum were taken into account. Due to the insufficient computer resources, we are restricted in this work to the use of a limited basis set.

The peaks 1–5 and 1′–5′ in the experimental spectrum [Fig. 4(d)] are assigned to the N_5 and N_4 groups, respectively.[2] Intensity distributions for the $N_5O_1O_{2,3}$ transitions predicted by the single-configuration picture [Fig. 4(a)] are in clear disagreement with experiment [Fig. 4(d)] as expected. The final states with $J=1$ gain most of the intensity, and thus the states $J=0,2$ are neglected in the further profiles. Figure 4(b) displays the redistribution of the intensity due to the correlation between the main (1,2) and satellite (3–5) lines. Final-state wave functions for the lines 1 and 2 show a clear $^3P_1$ and $^1P_1$ character such that the decomposition from the jj-coupled $5s^15\bar{p}^15p^4$ and $5s^15\bar{p}^25p^3$ states ($\bar{p}$ refers to $p_{1/2}$ and p to $p_{3/2}$) in intermediate-coupling resembles the one observed by the single-configuration approach. Due to the strong mixture of the $5s^15p^5$ and $5s^25p^35d^1$ configurations, the single-configuration assignment becomes questionable. The same assignment with the photoelectron results[11–17] makes the comparison easier, however, which is why we assign peaks 1 and 2 to main or parent and peaks 3–5 to satellite lines. This labeling is of purely notational value.

Line 3 is dominated by $^3P_1$ character and lines 4 and 5 by $^1P_1$ character. Line 3, however, shows a strong $^1P_1$ and $^3P_1$ mixing, so that its nomeclature is not clear. Comparison with the experimental $N_5O_1O_{2,3}$ transitions [peaks 1–5 in Fig. 4(d)] shows that the general agreement is good, although the energy splitting, especially that of line 3, is overestimated by theory. The intensity of line 3 is, furthermore, clearly underestimated. The intensity and position of line 3 was most strongly affected by the use of different kinds of limited basis sets in the calculations. Extension of the basis set to a full series of the $5s^25p^35d^1$ states in an average energy optimization level calculation with MCDF code[9] was found to give satellites too intense. The intensity of line 5 especially was found to increase too much. Extension to higher Rydberg and continuum states[16] would provide a better description. More theoretical work is thus needed in this area.

In Fig. 4(c), where we show the sum of the N_5 and N_4 groups to compare directly with experiment [Fig. 4(d)], displacement of line 3 causes the main disagreement with experiment in the satellite region. The main lines, with the overlap of $N_5O_1O_{2,3}(^3P_1)$ (1) and $N_4O_1O_{2,3}(^1P_1)$ (2′), are reproduced well by theory.

A much stronger correlation satellite structure (lines 3–5 and 3′–5′) clearly appears in the $N_{4,5}O_1O_{2,3}$ spectrum compared to the 5s photoelectron spectrum, as mentioned above. The satellite intensity relative to the parent intensity was estimated theoretically to be 0.55 in Ref. 13 for the 5s photoionization whereas a value of 1.0 was obtained experimentally in Ref. 4 in agreement with the theoretical prediction of Hansen.[17] For the Auger decay, our experimental satellite-to-parent ratio of 2.50 is obtained by taking the ratio of the averaged intensities of satellite (12–18.5 eV) and parent (18.5–24.5 eV) structures. The calculations, using a limited basis set, seem to underestimate the redistribution of the intensity, while the calculations using a full $5s^25p^35d^1$ basis set overestimate the satellite intensity. Therefore more careful calculations researching the influence of the basis set are needed.

Resonantly excited spectra

Excited resonance spectra at a 65.3- and 67.3-eV photon mean energies are shown in Figs. 1(b) and 1(c). They should be simpler than the normal $N_{4,5}$ spectra because only the N_5 or the N_4 spectrum appears after excitation of Xe to $4d^95s^25p^6(^2D_{5/2})6p$ or to $4d^95s^25p^6(^2D_{3/2})6p$ resonance states. However, both spectra show very complicated structures. Resonance states can decay by processes where one of the 5s or 5p electrons fills the 4d vacancy and another is ejected, the 6p electron remaining as a spectator. These resonance Auger processes with the excited electron as the spectator are often called spectator transitions. On the other hand, the 6p electron can participate in the transition. These autoionization processes involving the excited electron are alternatively referred to as participant decays. The final states for the participator processes are single-hole states where one electron is removed from an orbital. These states can be reached through the ordinary photoemission process, and the corresponding spectrum is the 5s and 5p photoelectron spectrum. Due to the overlap of the autoionization (with the excited electron as the participator) and photoelectron lines their intensity ratios cannot be distinguished. The final states of the resonance Auger spectra with the spectator electron can be reached also by the photoemission process and a simultaneous excitation of another electron to a higher state (shakeup). The correlation satellite structure accompanying the 5s photoelectron line falls in the same energy region as the resonance Auger lines, further complicating the analysis of the spectrum.

The resonance Auger spectra are found to shift and split due to the 6p spectator electron. This can be seen by comparing the experimental spectra in Fig. 1. For the $N_5O_{2,3}O_{2,3}$ transitions the shift was also experimentally observed and discussed in Ref. 5 and 6. In more detail, the shifts and extra splittings due to the coupling between the spectator electron and the electrons participating in the transition are demonstrated in Figs. 5 and 6, where the calculated profiles are compared with experiment. Figures 5(a) and 6(a) show the experimental $N_5O_{2,3}O_{2,3}$ and $N_4O_{2,3}O_{2,3}$ spectra following the $4d\rightarrow 6p$ excitation at 65.3- and 67.3-eV photon energies. As already pointed out by Schmidt,[6] in addition to the spectator transitions $4d^96p\rightarrow 4d^{10}5p^46p$, the shake-up transitions $4d^96p\rightarrow 4d^{10}5p^47p$ also occur with remarkable intensity. Furthermore, the rather large photon bandwidth (full width at half maximum, 0.6 eV) used in these measurements, and the uncertainty (± 0.2 eV) in our mean photon energy, may make the direct $4d\rightarrow 7p$ excitation possible. This leads to the spectator transitions $4d^97p\rightarrow 5p^47p$. The intensity ratios of different transitions can be estimated by comparing experiment with the calculated spectra in Figs. 5 and 6.

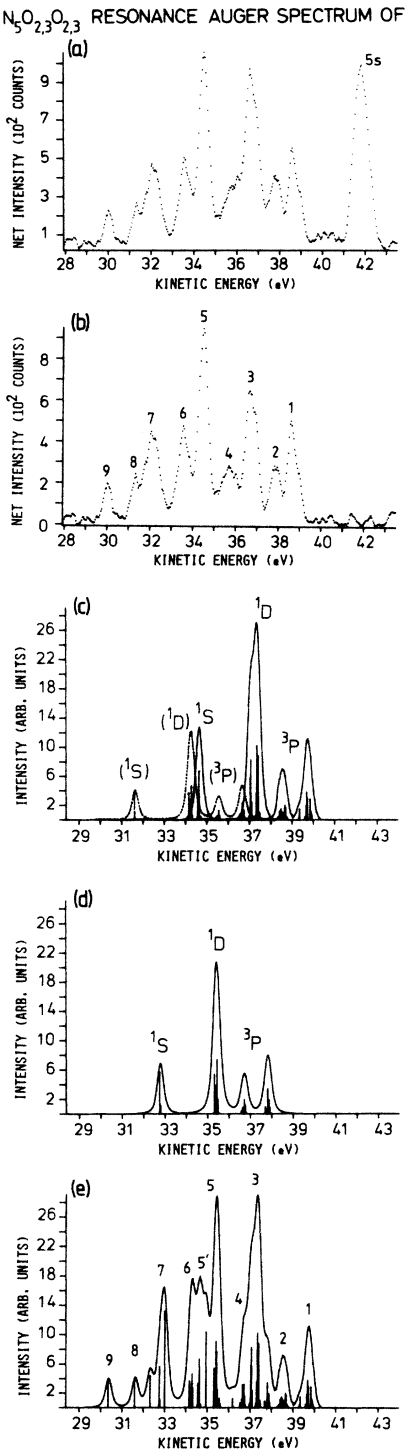

FIG. 5. (a) Experimental $N_5O_{2,3}O_{2,3}$ resonance Auger spectrum taken at (65.3±0.2)-eV photon mean energy, and (b) after subtraction of the 5*s* photoelectron spectrum shown in Fig. 2. Calculated (c) $4d^9_{5/2}6p \rightarrow 5p^4 6p$ (solid curve), $4d^9_{5/2}6p \rightarrow 5p^4 7p$ (dashed curve), and (d) $4d^9_{5/2}7p \rightarrow 5p^4 7p$ profiles. (e) Sum of profiles (c), (d), and normal $N_{4,5}O_{2,3}O_{2,3}$, as discussed in the text. Peak 5′ is due to the $4d^9_{5/2}6p \rightarrow 5p^4(^1S)6p$ decay, and peak 5 to the $4d^9_{5/2}7p \rightarrow 5p^4(^1D)7p$ decay. In experiment (a) these lines are expected to overlap at the position of line 5.

Before the comparison with experiment was done, the 5*s* photoelectron spectrum accompanied by the 5*s* and 5*p* satellite structure shown in Fig. 2 was subtracted from the experimental spectra [Figs. 5(b) and 6(b)]. Electron spectra recorded on and off resonances by Southworth *et al.*[4] showed no visible differences in the intensities of the 5*p*

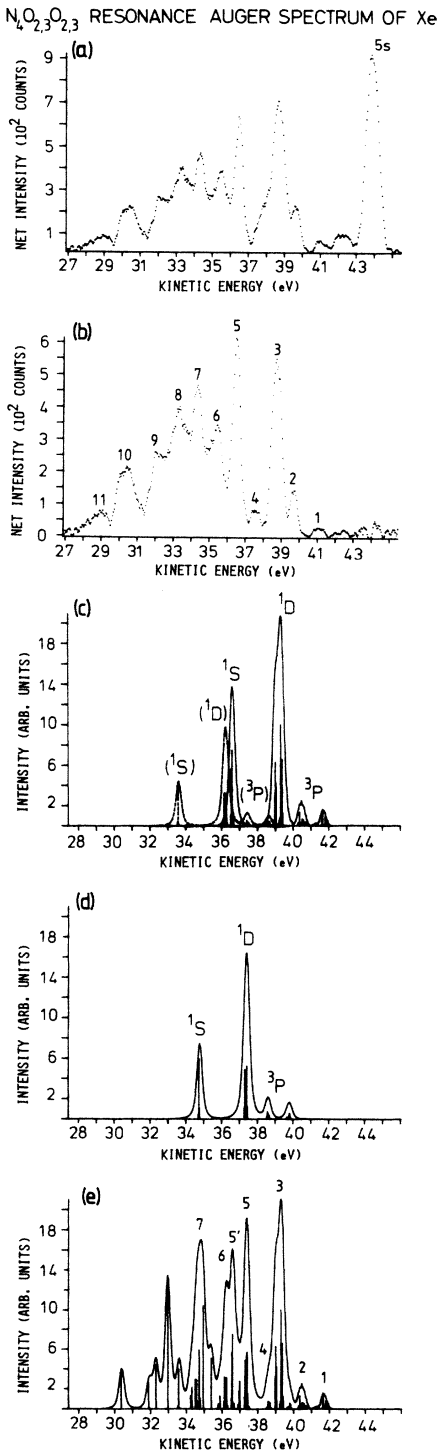

FIG. 6. $N_4O_{2,3}O_{2,3}$ resonance Auger spectrum at (67.3±0.2)-eV photon mean energy. See caption of Fig. 5 for detailed description. Sum profile (e) contains $4d^9_{5/2}8p \rightarrow 5p^4 8p$ spectrum too.

and 5s photolines. This indicates that autoionization involving the excited electron plays a minor role compared to the resonance Auger decay with the excited electron remaining as the spectator. Subtraction of the 5s photoelectron spectrum (Fig. 2) from the spectra shown in Figs. 5(a) and 6(a) thus results in the pure resonance Auger profiles [Figs. 5(b) and 6(b)]. This kind of subtraction, however, neglects the interference between the $5p^46p$ ($5s^15p^56p$) final state and the 5p (5s) photoelectron satellite lines resulting from ionization and 5p-6p shakeup. These effects thus remain in the spectra and only the nonresonance $5s^1$ and $5p^5$ satellite structure and the $5s^1$ correlation satellite structure is taken away. Interference effects were found to be negligible by Southworth *et al.*[4] Their findings can now be tested by comparing experiment with calculated structure, where the interference effects are neglected. A small amount of the normal $N_{4,5}O_{2,3}O_{2,3}$ Auger spectrum may be present in the experimental resonance spectra arising from ionization by second- and higher-order diffracted light and by scattered light in the photon beam. This was also taken into account when forming the sum profile. The spectrum of Fig. 6 obtained after excitation of Xe to the $4d^95s^25p^6(^2D_{3/2})6p$ resonance state at 67.3 eV shows a strong contribution of the N_5 Auger process after excitation to the $4d^95s^25p^6(^2D_{5/2})8p$ state too. Due to the near degeneracy of the $4d^95s^25p^6(^2D_{3/2})6p$ and $4d^95s^25p^6(^2D_{5/2})8p$ states it was not possible to produce a pure $4d_{3/2}\rightarrow 6p$ resonance excitation spectrum. The $4d_{5/2}\rightarrow 8p$ resonance excitation was taken into account when forming the sum profile for the N_4 resonance Auger process.

The strongest high-energy peaks in both the N_5 and N_4 resonance Auger spectra [number 3 in Figs. 5(b) and 6(b)] can be identified to correspond to those $4d^96p\rightarrow 5p^46p$ transitions, where the final states are the daughter levels of the $5p^4(^1D_2)$ parent, in the presence of a 6p spectator electron. The extra splitting caused by a spectator is most noticeable for the transitions to the $5p^46p$ states, as can be seen in Figs. 5(c) and 6(c), where the $4d^96p\rightarrow 5p^46p$ transitions are shown by the solid curve. This splitting is much smaller for the $5p^47p$ states. The $5p^47p$ final state may be populated either via the $4d^96p\rightarrow 5p^47p$ transitions [dashed lines in Figs. 5(c) and 6(c)] or by the $4d^97p\rightarrow 5p^47p$ transitions which follow the $4d\rightarrow 7p$ excitations [Figs. 5(d) and 6(d)]. The experimental results [peak 3 is considerably broader than peak 5 in Figs. 5(b) and 6(b)] are consistent with the theoretical results for the open-shell broadening. Experimentally, peak 3 is found to shift by 4.36 eV on going from the normal $4d^9_{5/2}\rightarrow 5p^4$ spectrum to the $4d^9_{5/2}6p\rightarrow 5p^46p$ spectator spectrum. The calculated shift of 4.37 eV is in excellent agreement. For the $4d^9_{3/2}\rightarrow 5p^4$ transitions, an energy shift of 4.34 eV is obtained by experiment as well as theory. Thus the energy shifts caused by the presence of a 6p spectator electron are reproduced very well by theory, even if the absolute energies are 0.65 eV larger than the experimental ones (Figs. 3, 5, and 6).

Peak 5 in Figs. 5(b) and 6(b) seems to fit energetically to the $4d^97p\rightarrow 5p^4(^1D_2)7p$ peaks shown in Figs. 5(d) and 6(d). For the N_5 group, an energy shift of 2.18 eV compared to the $4d^9_{5/2}\rightarrow 5p^4(^1D_2)$ line, obtained experimentally, agrees well with the calculated value of 2.37 eV. For the N_4 group, shifts of 2.14 and 2.40 eV are determined experimentally and theoretically, respectively. The $4d^97p\rightarrow 5p^4(^1D_2)7p$ lines overlap strongly with the $4d^96p\rightarrow 5p^4(^1S_0)6p$ lines. In the experimental spectrum, the overlap may even be larger than estimated by theory, because theory tends to overestimate the $^1S_0$-$^1D_2$ splitting (see Fig. 3). Higher measured intensity of peak 5 compared to peak 3, however, indicates that the $4d^96p\rightarrow 5p^4(^1S_0)6p$ decay cannot explain peak 5 alone, even if the energy splitting of peaks 3 and 5 is close to the $^1S_0$-$^1D_2$ splitting. Furthermore, our measured intensity of peak 5 is about twice as large as shown in Fig. 4 of Ref. 4. The high intensity and the good agreement between calculated and experimental energy shifts leads us to assume that peak 5 is, in addition to the $4d^96p\rightarrow 5p^4(^1S_0)6p$, also due to the $4d^97p\rightarrow 5p^4(^1D_2)7p$ transitions. In order to check the positions of the $4d^97p\rightarrow 5p^4(^1D_2)7p$ lines experimentally, both the $4d^9_{5/2}7p\rightarrow 5p^47p$ and $4d^9_{3/2}7p\rightarrow 5p^47p$ resonance Auger spectra were measured at photon energies 66.3 and 68.3 eV. Poor statistics made the handling of these spectra difficult, but the measurements clearly supported the appearance of the $4d^97p\rightarrow 5p^4(^1D_2)7p$ lines at the position of peak 5.

The $4d^96p\rightarrow 5p^4(^1D_2)7p$ transitions [main peak in the dashed curve in Figs. 5(c) and 6(c)] fit well energetically with peak 6. Theory predicts an energy shift of 1.27 eV between the $4d^9\rightarrow 5p^4(^1D_2)$ and $4d^16p\rightarrow 5p^4(^1D_2)7p$ transitions, whereas experimentally peak 6 is found to shift by 1.24 eV in the M_5 group and by 1.34 eV in the M_4 group.

Figure 5(e) shows a sum spectrum where relative-intensities of 100, 50, 30, and 30 were used for the $4d^9_{5/2}6p\rightarrow 5p^46p$, $4d^9_{5/2}7p\rightarrow 5p^47p$, $4d^9_{5/2}6p\rightarrow 4d^9_{5/2}7p$, and $4d^9\rightarrow 5p^4$ theoretical profiles, respectively. Comparison with Figs. 5(a) or 5(b) shows fairly good agreement in regard to the intensity distribution. The good agreement leads us to conclude that the interference effects between photoelectron satellites (strongest satellite lines located around peak 3) and resonance Auger lines do not play a strong role in the spectrum taken at 65.3 eV photon energy. The spectrum is well reproduced by transitions with 6p or 7p spectator electrons and has a significant amount of the shake-up $4d^9_{5/2}6p\rightarrow 5p^47p$ and the normal $4d^9\rightarrow 5p^4$ spectra. The agreement is surprisingly good, especially taking into account that the $^1S_0$ to $^1D_2$ splitting may be overestimated and intensity ratio underestimated by theory (Fig. 3). This may cause some uncertainty in the determination of fractions of different transitions at the low-kinetic-energy part of Fig. 5(a), beginning around peaks 5 and 6, where the $4d^9_{5/2}6p\rightarrow 5p^4(^1S_0)6p$ appears. However, an obvious portion of $4d^9_{5/2}7p\rightarrow 5p^47p$ type transitions is clearly present, although the sum in Fig. 5(e) may overestimate the portion. The uncertainty of our photon beam—we may not lie at the maximum of the $4d_{5/2}\rightarrow 6p$ excitation—and the large bandwidth may make the direct $4d_{5/2}\rightarrow 7p$ excitation possible. The $4d^9_{5/2}6p\rightarrow 5p^47p$ process, due to the $6p\rightarrow 7p$ shakeup during the Auger decay, is also suprisingly strong, as already pointed out by Schmidt.[6] The low-kinetic-energy regions

(7–9) show some amount of normal $4d^9 \rightarrow 5p^4$ transitions due to ionization by second-order light. Transitions which follow when shake off $6p \rightarrow \epsilon l$ takes place during the Auger decay may also appear in this region, but have not been taken into consideration.

For the resonance excitation spectrum taken at 67.3 eV photon energy (Fig. 6) the formation of the theoretical sum spectrum is more complicated. This is because the $4d_{5/2} \rightarrow 8p$ resonance excitation takes place at the same energy. An attempt to form a sum spectrum is presented in Fig. 6(e). Relative intensities of 100, 50, 30, 20, and 30 were used for the intensities of $4d^9_{3/2}6p \rightarrow 5p^4 6p$, $4d^9_{3/2}7p \rightarrow 5p^4 7p$, $4d^9_{3/2}6p \rightarrow 5p^4 7p$, $4d^9_{5/2}8p \rightarrow 5p^4 8p$, and $4d^9 \rightarrow 5p^4$, respectively. The low-kinetic-energy part of the spectrum is not very well reproduced by the calculated sum spectrum. This may be due to the differences in calculated and experimental energy splittings, which cause too strong overlap of lines in the theoretical spectrum. The effect tends to be more visible in the case, where the N_4 and N_5 groups overlap (compare with Fig. 3).

The $N_5O_1O_{2,3}$ and $N_4O_1O_{2,3}$ resonance Auger spectra shown in Figs. 7 and 8 have not been observed or analyzed before. The main $O_1O_{2,3}(^1P_1)$ peaks (2) are found to shift by 4.76 and 4.72 eV in N_5 and N_4 resonance spectra, respectively. These spectra are, indeed, very complicated. They show, in addition to the shifting, splitting effects and the shake-up structure observed for the $N_5O_{2,3}O_{2,3}$ and $N_4O_{2,3}O_{2,3}$ resonance spectra, the correlation satellite structure. Corresponding to the alternative assignment of double Auger transitions for the correlation satellites in the normal $N_{4,5}O_1O_{2,3}$ spectrum, we may designate the structure, on the low-kinetic-energy part of Figs. 7 and 8, as resonance double Auger transitions. To obtain a theoretical estimate for their profiles is a laborious task. Most difficulties arise because of the choice of the basis set, which must be extended from the one used in the previous section due to the open np shell. We were not able to choose a basis set which could give a satisfactory agreement with theory. The discrepancy caused by an unsatisfactory basis set could be eliminated by carrying out more careful calculations. They are, however, beyond our computer resources at the moment.

Figures 7(b) and 8(b) show the calculated profiles for the transitions from the $4d^9 6p$ initial to the final state which is a mixture of the $5s^1 5p^5 6p$ and $5s^2 5p^3 5d 6p$ configurations. As in Fig. 4(b) we see the main (1 and 2) and satellite (3–5) lines. The splitting between main and satellite lines is overestimated by theory, while the theoreti-

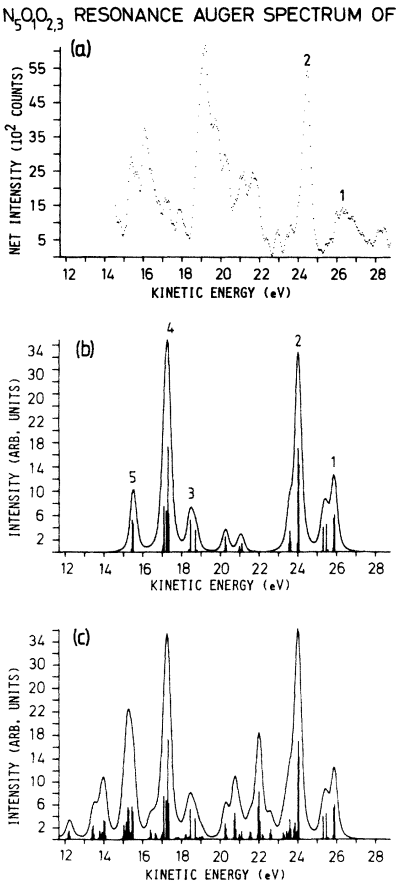

FIG. 7. $N_5O_1O_{2,3}$ resonance Auger spectrum taken with 65.3-eV photons (a) compared with the calculated $4d^9_{5/2}6p \rightarrow 5s^1 5p^5 6p \leftrightarrows 5s^2 5p^3 5d^1 6p$ profile (b) and with the sum profile (c).

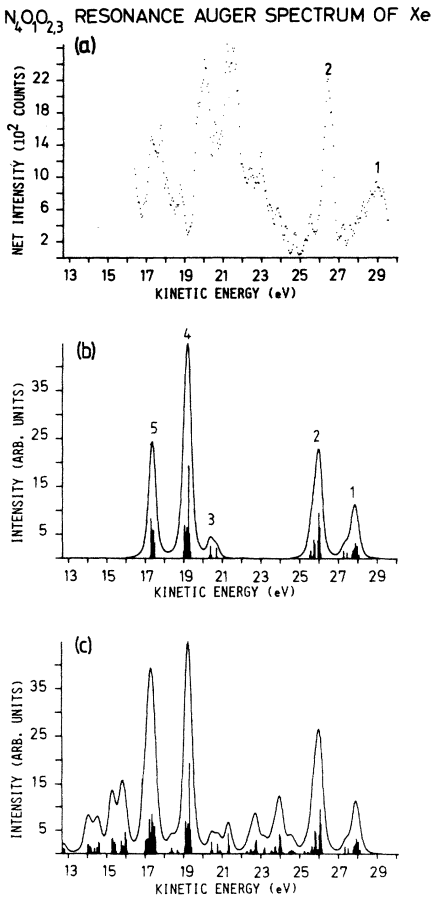

FIG. 8. $N_4O_1O_{2,3}$ resonance Auger spectrum with 67.3-eV photons (a) compared with the calculated $4d^9_{3/2}6p \rightarrow 5s^1 5p^5 6p \leftrightarrows 5s^2 5p^3 5d^1 6p$ profile (b) and with the sum profile (c).

cal satellite intensity is much less than observed. Figure 7(c) presents the sum profile of the $6p$ and $7p$ spectator and $6p \rightarrow 7p$ shake-up transitions for the N_5 group. The same ratios for the different transitions as obtained for the $N_5O_{2,3}O_{2,3}$ resonance spectrum were used. Although the calculations are unable to fully reproduce the observed structure, they help to assign the experimental peaks. High-kinetic-energy lines 1 and 2 at 23–27.5 eV are due to the main lines $4d^9_{5/2}6p \rightarrow 5s^15p^5(^1P_1,^3P)6p$. The satellites accompanying them lie in the region 18–23 eV, overlapping with the $4d^9_{5/2}7p \rightarrow 5s^15p^5(^1P_1,^3P)7p$ and $4d^9_{5/2}6p \rightarrow 5s^15p^5(^1P_1,^3P)7p$ main lines. Satellites following these main lines again appear in the 15–18-eV region. The low-kinetic-energy part of Fig. 7(a) also has some contributions from the $N_{4,5}O_1O_{2,3}$ normal Auger transitions, which were not taken into the sum of Fig. 7(c).

It is very interesting to follow the strength of the correlation satellites in going from the normal $N_{4,5}O_1O_{2,3}$ spectrum to the resonance spectra. This is because the intensity distribution between main and satellite lines was found to be sensitive to the states of the other electrons in a comparison between photoelectron and Auger electron studied discussed above. Because of the overlap of the $4d^9_{5/2}6p \rightarrow 5s^15p^56p$ satellite and $4d^9_{5/2}7p \rightarrow 5s^15p^57p$ and $4d^9_{5/2}6p \rightarrow 5s^15p^57p$ main lines, difficulties arise in the determination of the experimental satellite to main line intensity ratio. We estimate the ratio to be 2.1 ± 0.2, which is slightly less than obtained for the $N_{4,5}O_1O_{2,3}$ normal transitions.

An analogous structure as for the $N_5O_1O_{2,3}$ resonance transitions, but shifted by the $5p_{5/2}$-$5p_{3/2}$ spin-orbit splitting of 1.96 eV, can be seen in the case of the $N_4O_1O_{2,3}$ resonance transitions (Fig. 8). For this spectrum, agreement between experiment and theory seems to be of the same order as for the $N_5O_1O_{2,3}$ resonance Auger process. The low-kinetic-energy part of Fig. 8(a) contains also the normal $N_{4,5}O_1O_{2,3}$ spectrum and the $4d^9_{5/2}8p \rightarrow 5s^15p^58p$ transitions, which have not been summed in Fig. 8(c).

The $N_5O_1O_1(^1S_0)$ line at 8.30 eV kinetic energy is found to shift by 4.68 eV with the $6p$ spectator, and the $N_4O_1O_1(^1S_0)$ line at 10.27 eV by 4.71 eV. Strong transfer of the intensity to the satellites, due to the mixing with the $5s^15p^45d^1$ and $5s^25p^25d^2$ configurations, lying about 10 eV on the low energy side of main lines, is estimated by theory. It has not been possible to confirm this experimentally, because the transmission of the spectrometer may decrease rapidly at very low kinetic energies.

So far we have examined the decay of the $4d^96p$ resonance state, which results in an emission of one Auger electron. The final state of the process, having an np spectator electron in the presence of two inner holes, may further Auger decay. The spectator electron can now participate in the process, which results in the emission of the second Auger electron. We thus deal with a true double Auger process. Following it, the atom is left in the doubly ionized configuration $5s^25p^4$ or $5s^15p^5$. According to the single-configuration Dirac-Fock predictions, the structures due to the double Auger process, lie 6.5–7 eV lower in energy as compared to the lines of the $6p$ spectator Auger process. The structures start to appear, for instance, around peak 9 in the $NO_{2,3}O_{2,3}$ resonance spectra of Figs. 5(b) and 6(b). These structures, which are hardly distinguishable from the background, were discussed more minutely in a new work,[18] which came to our attention while this work was under final revision. According to the analysis of this work, the spectator and shake-up transitions form, however, the main peaks of the resonance spectra, in agreement with our analysis.

CONCLUSIONS

The high-resolution $N_{4,5}OO$ normal and resonantly excited Auger spectra of Xe have been studied by comparing calculated profiles with measurements carried out using synchrotron radiation. Resonance Auger spectra at $4d_{5/2} \rightarrow 6p$ and $4d_{3/2} \rightarrow 6p$ excitations show, in addition to the $6p$ spectator decay, strong structures due to shake-up transitions to $5p^47p$ final states. The spectator decay $4d^97p \rightarrow 5p^47p$ also appears due to direct $4d \rightarrow 7p$ excitation. Autoionization involving the excited electron plays a minor role and the excited states mainly decay by the spectator Auger process.[4] Interference effects with the $5p \rightarrow 6p$ shake-up satellites of the $5p$ and $5s$ photolines are negligible. Theory predicts very well the energy shifts due to the spectator electron. Intensity distributions in the normal $N_{4,5}O_{2,3}O_{2,3}$ and especially in the $N_5O_{2,3}O_{2,3}$ and $N_4O_{2,3}O_{2,3}$ resonance Auger spectra are well reproduced by the single-particle calculations. The multiconfiguration approach, on the other hand, is needed to interpret the satellite structure of the $NO_1O_{2,3}$ and NO_1O_1 transitions. The satellite-to-parent ratio and energy difference is found to be very sensitive to the states of the other electrons. The $N_5O_1O_{2,3}(^1P_1)$ line is shifted by 4.76 eV on passing from a normal to resonance spectrum, whereas the shift of 4.36 eV was observed for the $N_5O_{2,3}O_{2,3}(^1D_2)$ line. Change in the correlation energy shift in the case of the $N_5O_1O_{2,3}$ transitions, on passing from a normal spectrum to the Auger spectrum with a spectator electron, is present in the former but absent in the latter shift value. The $NO_1O_{2,3}$ normal and resonance Auger spectra provide a powerful area to study correlation effects. More theoretical work, especially to research the influence of the basis set, is needed in this area.

ACKNOWLEDGMENTS

We would like to acknowledge financial support from the National Research Council of Canada (NRC), the Natural Sciences and Engineering Research Council of Canada (NSERC), the University of Western Ontario, and the Finnish Academy of Science. We would also like to acknowledge the assistance of B. W. Yates and L. L. Coatsworth, and the helpful advice and assistance of the staff at the Synchrotron Radiation Center (Stoughton).

*Permanent address: Department of Physics, University of Oulu, SF-90570 Oulu 57, Finland.

[1]L. O. Werme, T. Bergmark, and K. Siegbahn, Phys. Scr. **6**, 141 (1972).

[2]H. Aksela, S. Aksela, and H. Pulkkinen, Phys. Rev. A **30**, 865 (1984).

[3]B. W. Yates, K. H. Tan, L. L. Coatsworth, and G. M. Bancroft, Phys. Rev. A **31**, 1529 (1985).

[4]S. Southworth, U. Becker, C. M. Truesdale, P. H. Kobrin, D. W. Lindle, S. Owaki, and D. A. Shirley, Phys. Rev. A **28**, 261 (1983).

[5]W. Eberhardt, G. Kalkoffen, and C. Kunz, Phys. Rev. Lett. **41**, 156 (1978).

[6]V. Schmidt, S. Krummacher, F. Wuilleumier, and P. Dhez, Phys. Rev. A **24**, 1803 (1981).

[7]K. H. Tan, P. C. Cheng, G. M. Bancroft, and J. Wm. McGowan, Can. J. Spectrosc. **29**, 134 (1984).

[8]C. D. Akers, C. Pathe, J. J. Barton, F. J. Grunthaner, P. J. Grunthaner, J. D. Klein, B. F. Lewis, J. M. Rayfield, R. Ritchey, R. P. Vasquez, and J. A. Wurzbach, CRUNCH user's manual (California Institute of Technology, Pasadena, California, 1982).

[9]I. P. Grant, B. J. McKenzie, P. H. Norrington, D. F. Mayers, and N. C. Pyper, Comput. Phys. Commun. **21**, 207 (1980); **21**, 233 (1980).

[10]E. J. McGuire, Sandia Research Laboratory Research Report No. San-75-0443 (unpublished).

[11]M. Y. Adam, F. Wuilleumier, N. Sandner, W. Schmidt, and G. Wendin, J. Phys. (Paris) **39**, 129 (1978).

[12]K. T. Leung and C. E. Brion, Chem. Phys. **82**, 87 (1983).

[13]K. G. Dyall and F. P. Larkins, J. Phys. B **15**, 203 (1982); **15**, 219 (1982).

[14]A. Fahlman, M. O. Krause, T. A. Carlson, and A. Svensson, Phys. Rev. A **30**, 812 (1984).

[15]J. E. Hansen, Commun. At. Mol. Phys. **12**, 1974 (1982).

[16]H. Smid and J. E. Hansen, J. Phys. B **16**, 3339 (1983).

[17]J. E. Hansen and W. Persson, Phys. Rev. A **18**, 1459 (1978).

[18]U. Becker, T. Prescher, E. Schmidt, B. Sonntag, and H.-E. Wetzel (unpublished).